

Fiducial cross-section measurements of top-quark pair production in association with a photon at $\sqrt{s} = 13$ TeV with the ATLAS detector

JOSHUA WYATT SMITH

on behalf of the ATLAS collaboration

*II. Physikalisches Institut
Goerg-August Universität, Germany*

Top-quark pairs in association with final state particles are produced in large quantities at the LHC due to the high centre-of-mass energy available in proton-proton collisions. One such topology is that of a prompt photon radiated from the top quark in addition to the final state particles from the top quark decay. Using 36.1 fb^{-1} of data collected at $\sqrt{s} = 13$ TeV with the ATLAS detector, fiducial cross-section results are shown in the single-lepton and dilepton channels. Object-level and event-level neural networks are used to increase sensitivity.

PRESENTED AT

11th International Workshop on Top Quark Physics
Bad Neuenahr, Germany, September 16–21, 2018

Copyright 2019 CERN for the benefit of the ATLAS Collaboration. Reproduction of this article or parts of it is allowed as specified in the CC-BY-4.0 license.

1 Introduction

The production of a top-quark pair in association with a photon is a direct probe of the electromagnetic coupling of the top quark. Possible anomalous top-quark couplings could manifest as shape discrepancies in various kinematic distributions or in cross-section measurements [1, 2]. The results can also be interpreted in the framework of an effective field theory in the search for new physics [3]. Photons can be radiated from all charged particles, including those in top quark decay and incoming initial state quarks. Kinematic cuts are applied to reduce the contribution of photons being radiated from top quark decay.

Previous studies have measured the cross section in the single-lepton channels [4–7]. In the analysis [8] summarised here, the fiducial cross sections are measured in the single-lepton channels and, for the first time, the dilepton channels. No distinction is made between electrons and muons from tau lepton decays. The measurements are performed using the ATLAS [9] detector at the LHC and a total dataset corresponding to 36.1 fb^{-1} , collected in 2015 and 2016 at a centre-of-mass energy of 13 TeV. Dedicated k -factors applied to the leading-order signal sample allow to compare the extracted cross sections to the next-to-leading order (NLO) theoretical calculations [10].

2 Signal region definition

Event selections are made to enhance the purity of the $t\bar{t}\gamma$ signal. Electrons are required to have $p_T > 25 \text{ GeV}$ ($p_T > 27.5 \text{ GeV}$) for the 2015 (2016) data, while muons are required to have $p_T > 27.5 \text{ GeV}$ for the 2015 and 2016 data. Only one reconstructed lepton is required for the single-lepton channels, while exactly two leptons of opposite sign are required for the dilepton channels. Electrons and muons are both required to be isolated based on calorimeter and track information. At least four (two) jets are required in the e +jets and μ +jets (ee , $e\mu$ and $\mu\mu$) channels. At least one of these reconstructed jets should be tagged as a b -jet with a working point efficiency of 77%. In all the dilepton channels a minimum invariant mass between the two leptons is such that $m(l, l) > 15 \text{ GeV}$. In the ee and $\mu\mu$ channels values of the invariant mass of the two leptons close to the mass of the Z -boson are vetoed, such that $m(l, l) \notin [85, 95] \text{ GeV}$. The same requirement is applied to the invariant mass of the system of the lepton pair and photon, $m(l, l, \gamma)$. In the ee and $\mu\mu$ channels a cut on the missing transverse energy of an event is required to be above a threshold, $E_T^{\text{miss}} > 30 \text{ GeV}$. In the e +jets channel a veto is placed on the invariant mass of the photon and the electron such that $m(\gamma, e) \notin [85, 95] \text{ GeV}$. In all channels, exactly one photon of $p_T > 20 \text{ GeV}$ is required. This photon needs to be isolated. A final cut is applied on the ΔR distance between the photon and the leptons, $\Delta R(\gamma, l) > 1.0$. This cut reduces the contribution of photons from top quark decay products.

The fiducial phase space is defined at particle level such that it mimics the above event selection, with the exception of the invariant mass veto cuts and the E_T^{miss} cuts that are only intended to suppress the background.

3 Background processes

The main background in the single-lepton channels consists of photons which are misidentified as electrons, the so-called “ $e \rightarrow \gamma$ fake” background. This occurs mainly from the $t\bar{t}$ dileptonic decays,

specifically from the $e\mu$ and ee channels. This background is negligible in the dilepton channels. Scale factors derived from a data-driven *tag-and-probe* method are used to correct the number of fake photons predicted by the Monte Carlo (MC) samples.

Photons from hadrons, or hadrons misidentified as photons make up the “hadronic fake” background. The majority of hadronic fake photons comes from $t\bar{t}$ events. Small contributions arise from W/Z +jets and single-top quark processes. Scale factors to correct MC prediction to data are derived in the single-lepton channel using the “ABCD” method. These are extrapolated to the dilepton channels.

Events with non-prompt leptons as well as fake leptons may satisfy the event selections for the signal region. These are categorised as “fake lepton” background. The main contribution comes from the QCD driven multi-jet processes in association with a photon. The estimation of the fake lepton background in the single-lepton channels follows the fully data-driven Matrix Method approach. In the dilepton channels this contribution is negligible.

Events in which a real prompt photon is radiated from anything except top quarks (or incoming quarks) make up the “Other prompt” background. For the single-lepton channel this is largely due to the $W\gamma$ process, whereas for the dilepton channel the main contribution is from the $Z\gamma$ process. Other processes such as single-top, diboson and $t\bar{t}V$, where each has an additional prompt photon in the final state, have small or even negligible contributions. In the single-lepton (dilepton) channels the $W\gamma$ ($Z\gamma$) contribution is largest and is therefore separated from the rest of the prompt photon backgrounds. The “Other prompt” background is estimated using MC.

4 Analysis Strategy

Object-level and event-level neural networks (NNs) are used to improve the sensitivity of the measurement in the single-lepton channels, while only an event-level NN is used in the dilepton channels. All NNs are implemented based on a feedforward architecture in the Keras [11] framework using the Theano [12] backend. The LWTNN [13] library is used to inject the trained NNs back into the ATLAS software framework. The object-level NN, called the Prompt Photon Tagger (PPT), is trained on independent prompt photon and di-jet samples, using information from the calorimeters. This NN serves to distinguish between prompt photons and hadronic fake photons. In the case of the single-lepton channel, the PPT distribution is then used as an input into the event-level NN, called the Event-Level Discriminator (ELD). The single-lepton (dilepton) ELD is trained using 15 (7) variables. For the single-lepton ELD, information about the b -tagged jet and the PPT proves to provide the most powerful variables. For the dilepton ELD, the b -tagged jet and the invariant mass of the two leptons prove to be very powerful. Examples of other variables used in the training include the $E_{\text{T}}^{\text{miss}}$, p_{T} of various jets and $m_{\text{T}}(W)$ (for the single-lepton channel).

The fiducial cross sections for each channel are extracted by performing a maximum likelihood fit to the ELD distribution. The cross section (σ_{fid}) is related to the number of signal events by

$$N_i^s = \mathcal{L} \times \sigma_{\text{fid}} \times C \times f_i^{\text{ELD}}, \quad (1)$$

where \mathcal{L} is the integrated luminosity, C is the ratio of all simulated events passing event selections to those only falling into the fiducial phase space, and f_i^{ELD} is the fraction of events falling into bin i of the ELD.

5 Results

Eight cross-section measurements are extracted from a maximum likelihood fit in the single-lepton, dilepton and combined channels. The post-fit ELD distributions for two of the measurements (the single-lepton and dilepton channel) are shown in Figure 1, where good agreement can be seen between MC and data points. The ELD distributions for other channels look similar. Table 1 shows the effects that groups of systematic uncertainties have on the fiducial cross-section measurements. In the single-lepton channel, the largest contributions come from the modelling of jets, the backgrounds, and the PPT. In the dilepton channel, signal and background modelling have the largest effect, but are generally still small.

The eight extracted cross sections are summarised in Table 2. In summary, all measurements are in agreement with NLO predictions.

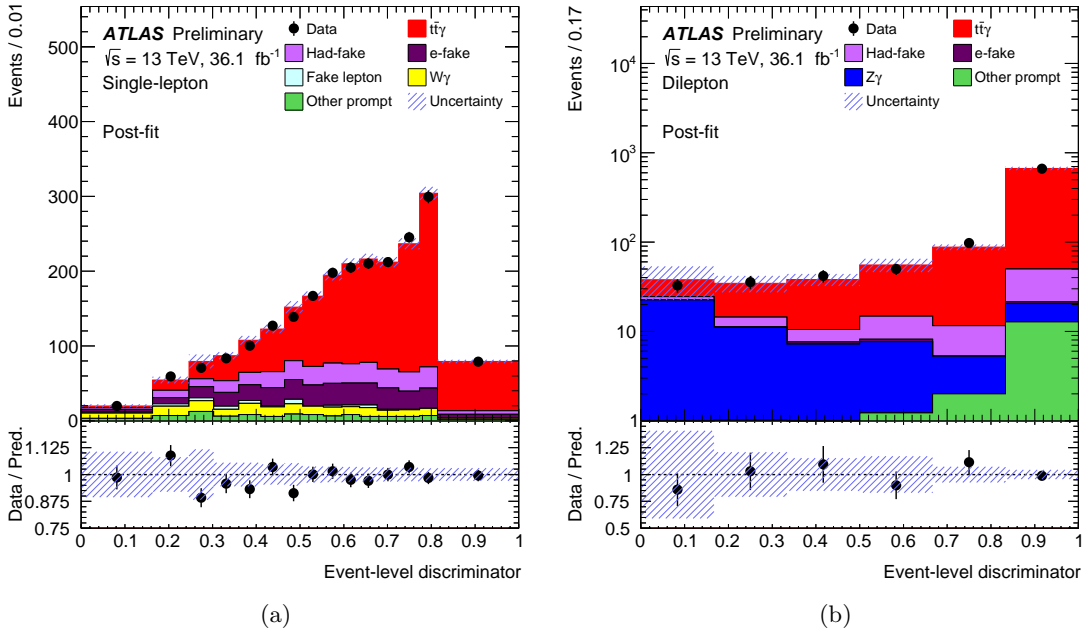


Figure 1: The post-fit ELD distributions for the (a) single-lepton and (b) dilepton channels. All the systematic uncertainties are included [8].

Source	Single lepton (%)	Dilepton (%)
Signal modelling	± 1.6	± 2.9
Background modelling	± 4.8	± 2.9
Photon	± 1.1	± 1.1
Prompt-photon tagger	± 4.0	-
Leptons	± 0.3	± 1.3
Jets	± 5.4	± 2.0
b -tagging	± 0.9	± 0.4
Pile-up	± 2.0	± 2.3
Luminosity	± 2.3	± 2.3
MC sample size	± 1.9	± 1.7
Total systematic uncertainty	± 7.9	± 5.8
Data sample size	± 1.5	± 3.8
Total uncertainty	± 8.1	± 7.0

Table 1: Summary of the effects of the groups of systematic uncertainties on the fiducial cross section in the single-lepton and dilepton channels [8].

Channel	$\sigma_{t\bar{t}\gamma}^{\text{fid}}$ [fb]	
	Measured $\pm(\text{stat.}) \pm(\text{syst.})$	Theory $\pm(\text{total})$
e +jets	$265 \pm 6 \pm 21$	247 ± 49
μ +jets	$250 \pm 7 \pm 22$	248 ± 50
ee	$16 \pm 2 \pm 2$	16 ± 2
$\mu\mu$	$18 \pm 1 \pm 2$	16 ± 2
$e\mu$	$34 \pm 2 \pm 2$	31 ± 5
Single-lepton	$521 \pm 9 \pm 41$	495 ± 99
Dilepton	$69 \pm 3 \pm 4$	63 ± 9
Inclusive (5 channels)	$589 \pm 10 \pm 34$	558 ± 110

Table 2: Fiducial cross-section summary for all channels, as well as theoretical predictions [8].

References

- [1] U. Baur, A. Juste, L. H. Orr, and D. Rainwater, Phys. Rev. **D71** (2005) 054013.
- [2] A. O. Bouzas and F. Larios, Phys. Rev. **D87** (2013) 074015.
- [3] O. Bessidskaia Bylund et al., JHEP **05** (2016) 052.
- [4] CDF Collaboration, Phys. Rev. **D84** (2011) 031104.
- [5] ATLAS Collaboration, Phys. Rev. **D91** (2015) 072007.
- [6] CMS Collaboration, JHEP **10** (2017) 006.
- [7] ATLAS Collaboration, JHEP **11** (2017) 086.
- [8] ATLAS Collaboration. ATLAS-CONF-2018-048, 2018, <http://cds.cern.ch/record/2639675>.
- [9] ATLAS Collaboration, JINST **3** (2008) S08003.
- [10] K. Melnikov, M. Schulze, and A. Scharf, Phys. Rev. D **83** (2011) 074013.
- [11] F. Chollet et al., *Keras*, <https://keras.io>, 2015.
- [12] Theano Development Team, ArXiv e-prints 1605.02688 (2016).
- [13] D. H. Guest, et al., 2017. <https://doi.org/10.5281/zenodo.290682>.